Influence of Ice Particle Shape on Albedo and Transmittance of Ice-Crystal Clouds

A. G. Petrushin
Institute of Experimental Meteorology
Obninsk, Russia

T. B. Zhuravleva
Institute of Atmospheric Optics
Tomsk, Russia

Introduction

Numerous experimental and theoretical studies indicate that the single-scattering properties of nonspherical ice cloud particles can differ substantially from those of surface- or volume-equivalent spheres (e.g., Volkovitskiy et al. 1984; Takano and Liou 1989). These differences affect the relationship between ice cloud microphysical properties and cloud radiative properties and, consequently, the accuracy of climate model representations of cloud radiative feedbacks (Sun and Shine 1995).

Generally, the sensitivity of cloud radiative properties to ice particle shape is studied using a plane-parallel, horizontally homogeneous cloud model; whereas ice-crystal clouds of moderate optical depth and optically thin cirrus clouds are known to widely vary in horizontal (e.g., Baum et al. 1995). Therefore, to better understand and properly parameterize the radiative properties of real ice-crystal clouds, it is necessary to study the potential inhomogeneity effects on the radiative transfer. One approach to solving this problem has been proposed by Liou and Rao (1996), who discuss the relative importance of cirrus cloud finiteness and inhomogeneity on the radiative properties employing an analytical three-dimensional (3-D) extinction coefficient. The influence of effects, caused by the random geometry of cirrus clouds with fixed microstructure, on the mean fluxes of visible solar radiation was studied by Zhuravleva and Kassianov (1989). The present work concentrates on the study of the combined effect of random cloud geometry and ice particle shape on the mean albedo R and transmittance T of the crystal clouds.

Ice Particle Shapes and Scattering Properties

As is well known, the single-scattering properties of atmospheric ice crystals depend essentially on both particle shape, which ranges from relatively regular hexagonal particles to aggregates of those to highly complex polycrystals, and on the particle size distribution in clouds (Macke et al. 1998). In this study, we will only consider ice particles shaped as solid hexagonal plates and columns. Based on the Auer and Veal (1970) data, we approximate the plate crystal size spectrum by the gamma size distribution function

$$f_{pl}(d,h) = Ad^{\alpha}\exp(-d\alpha/d_{mod}),$$

where A is the normalization constant, and d_{mod} is the modal size of plates. We performed calculations using d_{mod} in the range 30 μm to 200 μm, and α in the range $\alpha = 6 \div 8$. Heymsfield and Platt (1984) have suggested that the size distribution of column-like ice crystals can be modeled for each temperature interval using one or two curves of the form

$$f_{col}(D,l) = Bl^{-\beta}\delta\left(D - \sum_{i=0}^{2} c_i l^i\right),$$

where B is the normalization factor, and c_i, i = 0,1,2, are coefficients in approximate expression relating length l to diameter D of column.

For ice plates with the shape factor $0.23 < c = h/d < 0.4$ and columnar crystals with $c = l/D < 3$, the chaotic orientation in the space predominates. Outside these ranges, the ice crystals have a preferred orientation in space, and, as found by Volkovitskiy et al. (1984), thin plates with $c \le 0.05$ and long columns with $c \ge 3$ are preferentially oriented in a fixed (horizontal) plane. Possible variations from this fixed horizontal orientation are within a few degrees for the plates and about 15° for columns.

Figure 1 shows scattering phase functions of ice-crystal clouds composed of randomly oriented plates and columns, calculated for wavelength 0.63 μm using the Petrushin (1998) method. The intercomparison performed here pertains to the case of nearly identical root-mean-square sizes R_2 (total surface

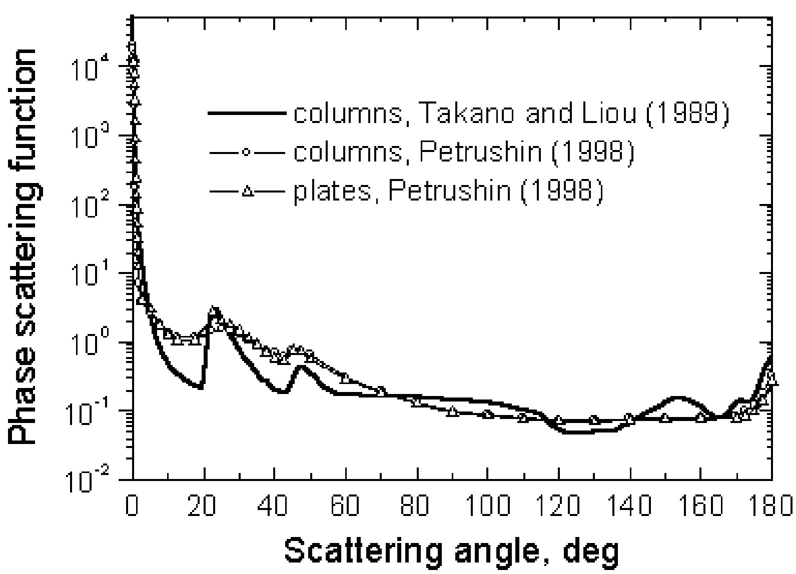

Figure 1. The scattering phase functions calculated at a visible wavelength λ = 0.63 μm for systems of ice plates and columns using the Petrushin (1998) method; and the scattering phase function of randomly oriented hexagonal columns presented by Takano and Liou (1989).

areas), being 19.7 μm for plates and 18.9 μm for columns. The phase functions for plates and columns substantially differ in the halo regions (at $\theta \approx 22°$ and 46°), at scattering angle $\theta \approx 140°$, and at back-scattering angles. In the halo region, the maximum for plates is shifted toward smaller scattering angles relative to that for the columns. In addition, the halo peak at $\theta \approx 22°$ is broader for columns than for plates. We note that the scattering phase functions presented here differ from those published by other authors, and the reasons for this are discussed by Petrushin (1998) in detail. Briefly, this may be both due to differences in the used scattering calculation techniques and particle size distribution functions. In particular, Takano and Liou (1989) calculated the scattering phase function using size distribution for hexagonal columns, including particles with a very large shape factor $c \approx 5$, for which the chaotic spatial orientation generally is not realized.

In the microstructure model of ice-crystal clouds considered here, the mean cosine of the scattering angle $\langle\mu_{pl}\rangle = 0.8$ for plates, and $\langle\mu_{pl}\rangle = 0.77$ for columns. The single scattering albedo is $\omega = 1$.

Radiative Effects of Ice-Crystal Clouds

In this section we present computational results for mean albedo R, diffuse transmittance Q_s, and angular distributions of upward and downward solar radiances for two cloud microstructure models outlined above. To characterize the mean angular distributions of upward (↑) and downward (↓) solar radiances, we use the quantity

$$\tilde{I}^{\uparrow(\downarrow)}(z_*,\mu_i,\mu_{i+1}) = \frac{1}{2\pi(\mu_{i+1}-\mu_i)} \times \int_{\mu_i}^{\mu_{i+1}} \int_{2\pi} I^{\uparrow(\downarrow)}(z_*,\mu,\varphi)\, d\varphi\, d\mu \,,$$

where $I(z,\mu,\varphi)$ is the mean scattered intensity in direction $\vec{\omega} = (\xi,\varphi)$, $\mu = \cos\xi$, at the level ($z = z_*$). The integration limits (μ_i,μ_{i+1}) are chosen such that the difference between the corresponding zenith angles would satisfy the relation $|\xi_i - \xi_{i+1}| = 5°$. In what follows, the subscripts "pl" and "col" will be used to denote the radiative characteristics calculated employing scattering phase functions for plate-like and column-like crystals, respectively. We will compare our results and results calculated using the scattering phase function for hexagonal columns suggested by Takano and Liou (1989) (subscript "TL").

A model of the cloudy-aerosol atmosphere and the Monte Carlo algorithm for calculating mean upward and downward fluxes of solar radiation are given in detail in Titov et al. (1997). It is assumed that a unit flux of solar radiation is incident on the top of the atmosphere in the direction $\vec{\omega} = (\xi_\oplus, \varphi_\oplus)$, where $\xi_\oplus$ and $\varphi_\oplus$ are zenith and azimuth solar angles. The underlying surface reflects according to Lambert law.

To estimate separately the influence of the scattering phase function of ice-crystal clouds on the mean angular distributions of upward and downward solar radiance at the cloud layer boundaries, we will calculate $\tilde{I}^{\downarrow(\uparrow)}$ in the horizontally homogeneous cloud model assuming that no beyond-cloud aerosol is present and that surface albedo $A_s = 0$ (Figure 2). As defined, $\tilde{I}^{\downarrow(\uparrow)}$ characterizes an average radiance over azimuth ($0 \le \varphi \le 2\pi$) and zenith ($\xi_{i+1} \le \xi \le \xi_i$) viewing angles; nevertheless, the angular

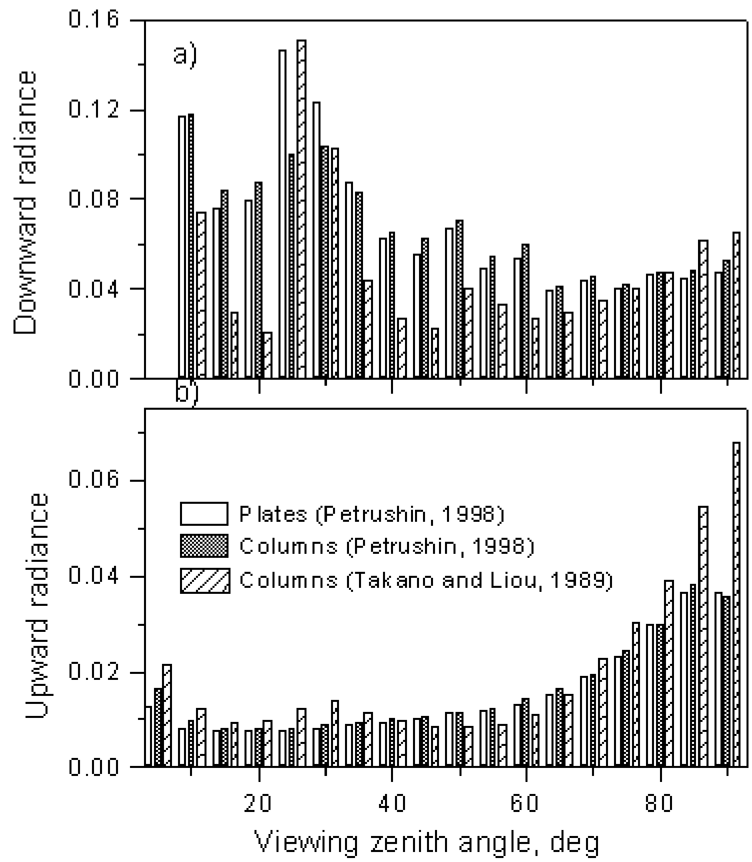

Figure 2. Angular distributions of (a) transmitted solar radiance at the bottom boundary and (b) reflected radiance at the top boundary of overcast, horizontally-homogeneous cloud layer with optical depth $\tau = 0.5$ under overhead sun $\xi_{\oplus} = 0$.

dependence of $\tilde{I}^{\downarrow(\uparrow)}$ well reflects the angular variations of the scattering phase functions (Figure 1) at small optical depths τ of ice clouds. In the transmitted radiance pattern, the 22° and 46° halo features produced by hexagonal particles are quite pronounced for all three phase functions considered here. In the 22° halo region, $\tilde{I}^{\downarrow}_{pl}$ for plates increases faster than $\tilde{I}^{\downarrow}_{col}$ for columns and becomes comparable to $\tilde{I}^{\downarrow}_{TL}$. For the other zenith viewing angles, $\tilde{I}^{\downarrow}_{pl}$ and $\tilde{I}^{\downarrow}_{col}$ are close in value and, with exception of $\xi \le 5°$ and $\xi > 80°$ ranges, they both exceed $\tilde{I}^{\downarrow}_{TL}$ everywhere. For upward solar radiance, $\tilde{I}^{\uparrow}_{pl}$ and $\tilde{I}^{\uparrow}_{col}$ differ insignificantly, except in observation directions close to nadir, the latter because the scattering phase functions for columns and plates differ at backscattering angles. Both $\tilde{I}^{\uparrow}_{pl}$ and $\tilde{I}^{\uparrow}_{col}$ differ from $\tilde{I}^{\uparrow}_{TL}$ primarily in that the latter has a maximum for $25° \le \xi \le 35°$, associated with the maximum of the scattering phase function at scattering angles between about 150° and 160° (Takano and Liou 1989).

Obviously, the larger τ and/or $\xi_\oplus$, the weaker the sensitivity of angular distributions to the shape of the scattering phase function of the ice-crystal clouds; e.g., at $\tau = 15$, the halo-associated features in angular distributions disappear.

Now let us explore how the shape and sizes of hexagonal particles influence the albedo R and diffuse transmittance Q_s of the ice-crystal clouds. The calculation results indicate that for overcast, horizontally homogeneous clouds with $\tau > 4$, the solar flux differences due to use of different cloud microstructure models are only minor. In optically thin clouds, R and Q_s exhibit larger differences; e.g., for the input model parameters used to calculate curves in Figure 3, the relative difference between albedos R_{pl} and R_{TL} is ≈10%.

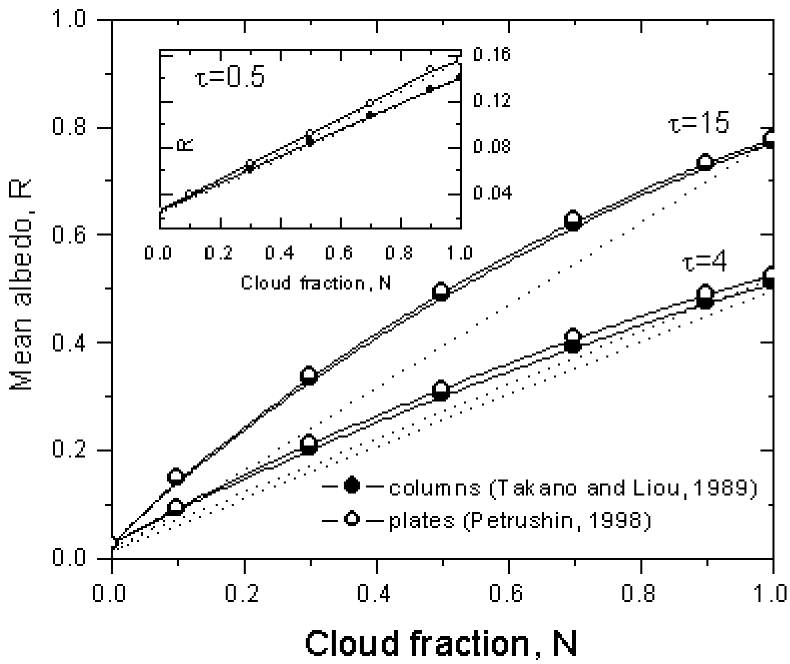

Figure 3. The mean albedo of the cloudy atmosphere calculated in the horizontally homogeneous (dots) and Poisson (solid lines) cloud models for $\xi_\oplus = 60°$, $\varphi_\oplus = 0$, $A_s = 0$, H = D_x = 2 km, and D_y = 100 km; the optical depth of the beyond-cloud aerosol $\tau_a = 0.15$.

However, the real clouds are known not to be always completely overcast. So, a relevant question to ask is how strongly do the shape and sizes of ice particles influence the radiative properties of the broken ice-crystal clouds? We consider a cloud field consisting of cloud bands with characteristic extents D_x and D_y along OX- and OY-axes, respectively. The band width D_x is assumed to be comparable with cloud geometrical thickness H and much less than the band length D_y. Such a spatial pattern is characteristic of the cirrus clouds and is frequently observed for A_s clouds.

We compared the mean radiative fluxes, calculated within horizontally homogeneous cloud model, to computations taking the effects of stochastic cloud geometry into account. It was found that 1) for optically thin clouds, the R and Q_s values are most sensitive to crystal shape and size; whereas 2) for clouds with optical depth $\tau > 4$ and intermediate cloud fractions N, the neglect of the horizontal inhomogeneity of real clouds leads to much larger errors in determining the mean radiative fluxes than when variations in ice-crystal cloud microstructure properties are ignored (Figure 3).

Conclusions

The present work considers the solar radiative transfer through ice-crystal clouds in a specific case when both variations in ice-particle shape and size are taken into consideration. The radiation calculations are made using data on the scattering properties of ice columns and plates computed by the methods of Petrushin (1998) and Takano and Liou (1989). It is shown that, in the optically thin clouds ($\tau \leq 1$), the angular distributions and fluxes of solar radiation depend strongly on the cloud microstructure model used in the calculations, and much less on the effects caused by the stochastic cloud geometry. In clouds with optical depth $\tau > 4$, the difference between radiation calculations performed with and without account of the random cloud geometry may reach tens of a percent, and exceeds considerably the bias due to the neglect of ice particle shapes and sizes.

References

Auer, A., and D. Veal, 1970: The dimension of ice crystals in natural clouds. *J. Atmos. Sci*., **27**, 919-926.

Baum, B. A., et al., 1995: Satellite remote sensing of multiple cloud layers. *J. Atmos. Sci*., **52**, 4210-4230.

Heymsfield, A. J., and G. M. Platt, 1984: A parameterization of the particle size spectrum of ice clouds in terms of the ambient temperature and ice water content. *J. Atmos. Sci*., **41**, 846-855.

Liou, K. N., and N. Rao, 1996: Radiative transfer in cirrus clouds; IV, On cloud geometry, inhomogeneity, and absorption. *J. Atmos. Sci.,* **53**, 3046-3065.

Macke, A., P. Francis, G. McFarquhar, and S. Kinne, 1998: The role of ice particle shapes and size distributions in the single scattering properties of Cirrus clouds. *J. Atmos. Sci*., **55**, 2874-2883.

Petrushin, A. G, 1998: Light scattering by hexagonal ice prisms. 2. Large (nondiffraction) scattering angles. *Izv. Russian Akad. Nauk, Ser. FAO*, **34**, 573-580.

Sun, Z., and K. P. Shine, 1995: Parameterization of cloud radiative properties and its application the potential climatic importance of mixed-phase clouds. *J. Clim*., **8**, 1874-1888.

Takano, Y., and K. N. Liou, 1989: Solar radiative transfer in cirrus clouds, I, Single-scattering and optical properties of hexagonal ice crystals. *J. Atmos. Sci*., **46**, 3-19.

Titov, G. A., T. B. Zhuravleva, and V. E. Zuev, 1997: Mean radiation fluxes in the near-IR spectral range: Algorithms for calculation. *JGR*, **102**, 1819-1832.

Volkovitskiy, O. A., L. N. Pavlova, and A. G. Petrushin, 1984: *Optical properties of crystal clouds*. Gidrometeoizdat, Leningrad.

Zhuravleva, T. B., and E. I. Kassianov, 1989: Mean radiative fluxes under conditions of broken cirrus clouds. In *Radiative properties of cirrus clouds*. Moscow, Nauka, p. 177-184.